SMART Rotor Development and Wind-Tunnel Test

Friedrich Straub, V.R. Anand, and Terry Birchette – The Boeing Company, Mesa, Arizona
Benton H. Lau – NASA Ames Research Center, Moffett Field, California

Summary

Boeing and a team from Air Force, NASA, Army, Massachusetts Institute of Technology, University of California at Los Angeles, and University of Maryland have successfully completed a wind-tunnel test of the smart material actuated rotor technology (SMART) rotor in the 40- by 80-foot wind-tunnel of the National Full-Scale Aerodynamic Complex at NASA Ames Research Center, figure 1.

The SMART rotor is a full-scale, five-bladed bearingless MD 900 helicopter rotor modified with a piezoelectric-actuated trailing-edge flap on each blade. The development effort included design, fabrication, and component testing of the rotor blades, the trailing-edge flaps, the piezoelectric actuators, the switching power amplifiers, the actuator control system, and the data/power system. Development of the smart rotor culminated in a whirl-tower hover test which demonstrated the functionality, robustness, and required authority of the active flap system.

The eleven-week wind tunnel test program evaluated the forward flight characteristics of the active-flap rotor, gathered data to validate state-of-the-art codes for rotor noise analysis, and quantified the effects of open- and closed-loop active-flap control on rotor loads, noise, and performance. The test demonstrated on-blade smart material control of flaps on a full-scale rotor for the first time in a wind tunnel. The effectiveness and the reliability of the flap actuation system were successfully demonstrated in more than 60 hours of wind-tunnel testing. The data acquired and lessons learned will be instrumental in maturing this technology and transitioning it into production.

The development effort, test hardware, wind-tunnel test program, and test results will be presented in the full paper. A brief description of the test hardware and test program is provided below.

Hardware and Test Program

The 34-foot diameter rotor has five composite blades with 10in chord and a 25% chord trailing-edge flap from 74 to 92% radius, figure 2. The flap is mounted to the blade using five equally spaced hinges. A piezoelectric actuator is installed in the blade spar at 74% radius. It drives the flap via a linkage that is connected to a horn at the inboard end of the flap. Rotor instrumentation includes a five-component balance, drive-shaft torque, and control-system motions. Blade load measurements include 8 flap, 6 chord and 6 torsion moments at various radial stations, as well as pitch link load. The piezoelectric actuator stroke, force, voltage and current are measured on each blade. All rotating-system measurements are acquired and multiplexed in a hub-mounted data system. The multiplexed data and the actuator control power are transmitted through a conventional 36-channel slip ring to the ground-station data system. Acoustic measurements include 4 fixed and 8 traversing microphones on the advancing side of the rotor disk. Acoustic data and wind-tunnel operating conditions are recorded by the NFAC wind-tunnel data system but rotor data are recorded by the Boeing data system.

The 11-week long wind-tunnel test was sponsored by DARPA and NASA. The objectives of the DARPA funded portion of the test were to acquire loads, performance, and acoustic data for an advanced rotor system in validating high-fidelity physics-based rotor-noise prediction tools that had

Abstract submitted for the 35th European Rotorcraft Forum, Hamburg, Germany, Sept. 22-25, 2009

been developed under the Helicopter Quieting Program (HQP). Test conditions for the validation included level-flight, descent, and high-speed cases with single and multiple harmonic flap inputs. Five test points were defined with speeds of 83, 123, and 155 knot. For each point the rotor thrust, the model pitch angle, the baseline (zero), and a flap-deflection schedule were specified. Flap inputs included amplitudes up to 3 deg at specified phasing and 2, 3 or 5/rev harmonic variation. All predictions were completed before the test. Data was successfully acquired at four test conditions. Blade loads were too high for the high-speed condition at 155 knot.

The primary objectives of the NASA funded portion of the test were to evaluate the effect of open- and closed-loop active flap control on rotor loads, noise, and performance. Open-loop flap inputs at 2 to 6/rev with fixed amplitude and phase sweeps were used to determine the optimum phase angle for noise reduction. Amplitude sweeps at optimal frequency and phase were then used to further reduce noise. For all noise test points, feedback of the actuator position was used to control the flap deflections precisely. Feedback of rotor-balance forces and moments was used for closed-loop control of vibrations. The impact of flap-control on rotor dynamics (modal identification) and flight controls (rotor response) was assessed by performing various open-loop flap frequency sweeps. The effectiveness of the active flap on control power and rotor smoothing (i.e. blade tracking) was evaluated using open-loop steady-state flap inputs. Test conditions included hover, descent and level flight cases at 62, 68, 82, and 124 knots.

The effectiveness of the active flap control on noise and vibration was conclusively demonstrated. Preliminary results show significant reductions in blade-vortex-interaction (BVI) and in-plane noise as well as vibratory hub loads. Up to 80% reduction in vibratory hub loads and up to 6dB noise reduction were measured. Trailing-edge flap deflections were controlled within 0.1 degrees of the commanded value. The impact of the active flap on control power and rotor smoothing was also demonstrated. Results illustrating the effectiveness of the active flap in various objectives noted above will be presented in the full paper. Sample results are discussed below.

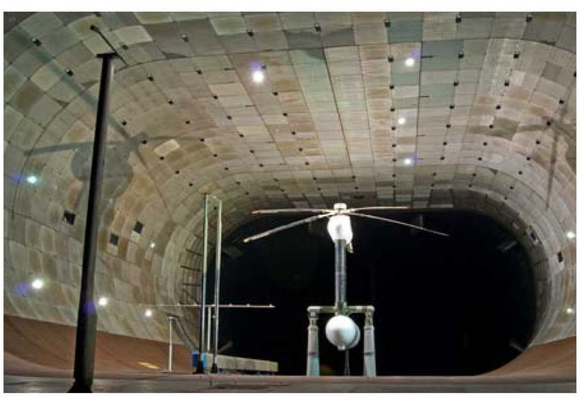

Figure 1: SMART rotor in the 40- by-80-foot wind tunnel of the National Full-Scale Aerodynamic Complex at NASA Ames Research Center.

Figure 2: Close-up view of the SMART rotor, blade, and flap